SEMI-AUTOMATIC DERIVATION OF DIGITAL ELEVATION MODELS FROM STEREOSCOPIC 3-LINE SCANNER DATA

M. Lehner (+), R.S. Gill (++)

(+) Deutsche Forschungsanstalt für Lu.. und Raumfahrt (DLR), Oberpfaffenhofen
(++) Computer Anwendung für Management GmbH (CAM), München

ABSTRACT

DLR is engaged in several stereo scanner projects (MEOSS on Indian Remote Sensing mission IRS-1E, MOMS-02 on German shuttle mission D2, HRSC and WAOSS cameras on Russian Mars mission). Besides fabricating the flight hardware for MEOSS camera DLR developed a software package for the evaluation of stereoscopic scanner data consisting of the following main subsystems:

Image matching software for automatically locating large numbers of conjugate points in 3-line stereo scanner imagery. It is based on areal matching in image pyramids and subsequent local least squares matching for subpixel positioning.

Photogrammetric adjustment software is used to derive digital elevation models and exterior orientation parameters. This combined point determination software is mainly based on collinearity equations for conjugate and ground control points. Further it allows for the constraining of the exterior orientation of the camera by given flight path and attitude data and by Gauß-Markov statistical processes.

The paper reports on the successful application of the software to airborne data taken with the satellite model of the MEOSS camera, including a comparison to an already existing DEM. Empirical and theoretical errors are given for various numbers of ground control points.

Keywords: 3-line stereo scanners, image matching, photogrammetry, digital elevation models

1. Introduction

DLR is engaged in stereo line scanner cameras since 1981, when the DLR Institute of Optoelectronics proposed to participate with a 3-line stereo camera (MEOSS: Monocular Electro-Optical Stereo Scanner) in an Indian satellite mission <Ref. 1>. Parallel to the manufacturing of the hardware, work on data analysis started with simulation of triple stereoscopic imagery, establishing image matching software and testing the photogrammetric adjustment process via simulation <Ref. 2-4>. Since 1986 an airborne model of the camera was available. This was the first time that a digital elevation model could be derived from such imagery <Ref. 5,7>. MEOSS is now scheduled for a flight on Indian satellite mission IRS-1E end of 1992. Airborne test data of the satellite flight model have been evaluated for this paper.

In contrast to MEOSS which is a single optics system, the stereo scanner MOMS-02 (Modular Optoelectronic Multispectral Scanner) being built by the German company Messerschmitt-Bölkow-Blohm (MBB) uses various optics of different focal lengths to take multispectral and stereoscopic images of the earth. This offers the possibility to derive digital elevation models and multispectral orthophotos of fine resolution for GIS-like applications. A description of the MOMS-02 scanner system can be found in <Ref. 6>. This scanner will be part of the payload of the German mission D2 now scheduled for a spaceshuttle flight in January 1993. One aim of the MOMS project is the development of a stereoscopic digital photogrammetric workstation in cooperation with several universities.

Other stereo scanner projects at DLR are the Mars-94/96 WAOSS and HRSC cameras <Ref. 11,12>. WAOSS (Wide-Angle Optoelectronic Stereo Scanner) is meant for global monitoring of Mars (pixel size on ground 150 m near periapsis) and for the derivation of global topography of Mars whereas HRSC (High Resolution Stereo Camera, 10-20 m pixel size) will allow the derivation of fine-grid digital elevation models together with orthophotos in several spectral channels. Both cameras are - like MEOSS - monocular instruments.

The derivation of digital elevation models from 3-line stereo scanner imagery consists of two main tasks:

- extraction of a large number of conjugate points from the stereoscopic imagery (image matching) and
- reconstruction of exterior orientation and calculation of the ground coordinates of the conjugate points via photogrammetric adjustment (combined point determination).

The location of conjugate points in triple stereoscopic line scanner imagery can be divided into the following steps:

- selection of patterns suitable for digital image correlation in the sense of an interest operator (the well-known Förstner operator is used)
- selection of search windows corresponding to these patterns in the images of the other looking directions
- digital image correlation (area based matching) to locate the pattern within the search area: image matching on pixel level
- subpixel refinement of the correlation result (done here by local least squares matching technique).

These steps are performed from level to level of an image pyramid in order to minimize manual interaction and to make the process more robust.

Iterative least squares techniques are used in photogrammetric adjustment based mainly on collinearity equations for conjugate and ground control points. Some other equations are used for the introduction of known platform flight path and attitude information and for the estimation of their constant and higher order biases. Interior orientation parameters can be estimated, too.

2. Image matching

2.1 Interest operator

In high resolution imagery like that from the airborne model of the MEOSS camera (about $2 \cdot 2m^2$ pixel size) large homogeneous areas like fields, meadows and water bodies appear where good patterns for image correlation cannot be extracted. Therefore, for automatic image matching, an interest operator has to automatically select patterns which are well suited for digital image correlation. Our interest operator is designed along the lines of the so-called "Förstner operator" developed at Stuttgart university <Ref. 8>.

The weighted centre of gravity is calculated for each window of a given size by least squares technique with appropriate weighting by first order derivatives in line and column directions. From the error ellipse of this least squares adjustment two parameters, *roundness* and *size*, are extracted. Windows and their resulting points are said to be promising for image correlation if the size is small and the roundness is beyond a given threshold so that the points are well defined in terms of multidirectional edge information contents of the surrounding window.

We found that the sizes of the error ellipses are correlated with the variances of the grey values of the windows (about -0.5 normalized correlation coefficient). Furthermore, it was found through many tests that windows - even if they meet the requirements on roundness and size described in <Ref. 8> - should have a variance beyond some threshold. Thus, for the user interface the threshold for size is replaced by a threshold for variance. This variance thresholds can be estimated from the local image variances much better than the median value of the sizes of the error ellipses mentioned in <Ref. 8>. For our airborne imagery thresholds between 25.0 and 64.0 for the variance gave reasonable distributions of the points found by the interest operator.

Normally, a promising point is located more than once by the operator (with respect to different windows). This multiplicity is reflected in our procedure via a count only. Huge numbers of points are registered often by this procedure. Thus, it is found a good strategy to replace a set of points which are lying near to each other by one prominent point. The selection of the prominent point is based on the following parameters, given in descending order of priority:

- multiplicity of point
- variance of window
- roundness of error ellipse
- size of error ellipse

2.2 Search window selection

The interest operator is used to locate good patterns in the nadir looking sensor's scene. For area based matching corresponding search areas have to be extracted from the scenes of the other looking directions. This is achieved by computing a local affine transformation between the stereo partners. The six parameters of the affine transformation are computed by least squares adjustment using already known conjugate points. Currently, at the lowest level of resolution of the image pyramid manually found conjugate points are used as input to this process. This could be further automated by using some a priori knowledge about the sensor geometry (e.g. stereo baselength in number of pixels) and interest operator results for **all** stereo partners.

The results of the local affine transformation are accepted only if the rms-error for the input conjugate points is less than half the possible shift of the pattern area within the search area. Thus, coarse errors in the position of the search windows are avoided. More trials are made by changing the number of input points and/or the the weighting scheme. If none of the adjustments is accepted no matching process for this point and stereo pair is initiated. The number and distribution of these affine transformation failures indicate to the user in what regions of the imagery the point densities for computing search area positions are not sufficient.

2.3 Image correlation with pixel accuracy

A matrix of normalized correlation coefficients is computed for given pattern and search areas by shifting the pattern pixel by pixel (in column and line directions) over the search area. The maximum of the correlation coefficients defines the location of that pixel in the search area which corresponds to the centre pixel of the pattern area. A quality figure is defined which measures the uniqueness and the relative steepness of the peak in the matrix of correlation coefficients (for definition see <Ref. 4>).

Strict acceptance rules are applied to the results

- of each individual correlation process between a stereo pair and
- of 3 combined correlation processes if 3 stereo pairs are available (in the zone of threefold stereoscopic coverage).

At the level of a single correlation the following conditions have to be met before acceptance of the results:

- maximum of correlation coefficients and quality figure have to be beyond given thresholds (in case of our data material 0.5 and 0.2 were taken for correlation coefficient and quality figure, respectively)
- the maximum of the correlation coefficient must not lie on the border of the matrix of correlation coefficients (the width of the border is normally set to 1 column and 1 line)

The latter condition is very helpful in regions with repetitive patterns.

For a full conjugate point where three stereo pairs are available the conditions are as follows:

- for all three correlations the above mentioned criteria for single correlations have to be fulfilled
- for the checking correlation between the backward/forward stereo pair the absolute value of the displacement vector resulting from the correlation must not exceed a given limit (normally set to 1 column and 1 line).

Pattern sizes have been 7 · 7 pixels for the 3 lower levels of the image pyramid and 9 · 9 for the two higher levels; accordingly, search area sizes of 15 · 15 and 21 · 21 were taken to cope with the increase in parallaxes at the higher levels. This is depending also on the density of the conjugate points found for the previous level of the image pyramid. Of course, high densities will help to reduce the search areas.

2.4 Subpixel accuracy

Local least squares matching techniques (LSM) described in <Ref. 9> are used to refine the results of the previously described operator to subpixel level. The radius of convergence of LSM is a few pixels only. Thus, it has to be preceded by a matching operator at pixel level.

The parameters of two local transformations between the stereo partners - two parameters of a radiometric transformation (brightness and contrast) and six parameters of an affine transformation for obtaining the subpixel positional information - are estimated by iterative least squares adjustment. The observations are the differences of the grey values of the original scene of the nadir looking sensor and the transformed subscene of the stereo partner. It was found that the convergence is bad for windows less than 11*11 pixels for the given data material (in <Ref. 9> 16*16 is recommended as smallest window size - but for frame camera imagery). The smoothing of the grey values before LSM mentioned in <Ref. 9> is not realized in our software because very good initial values are provided by correlation at pixel level.

For most windows the convergence is within 2 to 5 iterations. In case of non-convergence the location of the maximum of a parabolic fit to the neighbourhood of the maximum of the correlation coefficients is taken as a substitute. This also defines the initial values taken for the LSM.
Experience showed that the parabolic fit maxima will often differ much from the LSM results. Convergence of LSM was achieved in about 90% of the cases.

2.5 Image pyramid

Already our short strips of stereo imagery of MEOSS type are a massive amount of bytes on disk or subareas fitting to normal display screens. Additionally, distortions introduced by the terrain and the attitude variations of the aircraft are often very large even locally (even more than 100 pixels). Thus, manual starting of locating conjugate points would be a very tedious task.

These problems are much reduced by introducing a resolution pyramid. If we use factor 16 for the coarsest resolution (in both line and column direction) this results in small scenes fitting to modern display screens. Furthermore, as parallaxes are reduced by the same factor, the human operator will be able to quickly measure the small set of conjugate points required for starting the search area selection. All further steps of interest operator and image correlation work automatically through the image pyramid up to the finest level of resolution.

The quality of the final results is profiting much from the fact that from one level of resolution to the next the increase in distortions is relatively small. Of course, one has to pay for this by an increase in computer time and disk storage (though a full pyramid of five levels results in a storage increase by a factor 1.33 only).

3. Photogrammetric combined point determination

3.1 Basic equations

The iterative least squares adjustment for computing the ground coordinates of the conjugate points and improved values of the exterior orientation parameters is based on the following types of equations:

- collinearity equations connecting image coordinates and ground coordinates of the conjugate points with the exterior orientation of the camera at certain orientation images
- observation equations for ground control points
- observation equations for the parameters of interior orientation of the camera (position of principal point and focal length)
- observation equations for exterior orientation parameters including constant and higher order biases
- a second order Gauss-Markov process for the parameters of exterior orientation (this is meant primarily for bridging large gaps in the distribution of conjugate points caused for example by large homogeneous areas, water bodies and clouds).

The exterior orientation is calculated for a set of orientation images. These may be selected with regular or irregular spacing in time along the orbit. Currently, linear interpolation is used to obtain the exterior orientation for each line of the scanner imagery <Ref. 2,10>. Thus 12 parameters of exterior orientation enter into the two collinearity equations derived for one imaging ray.

3.2 Input data

The input to the photogrammetric adjustment consists of:

- the conjugate points found by semi-automatic image matching (these are the most precise measurements)
- ground control points: these are conjugate points which are also identified on maps; topographic maps are used to extract Gauß-Krüger coordinates and heights (this is a very tedious and time consuming manual work)
- initial values for the exterior orientation at the orientation images
- geometric calibration data for the camera
- weights for all the error equations.

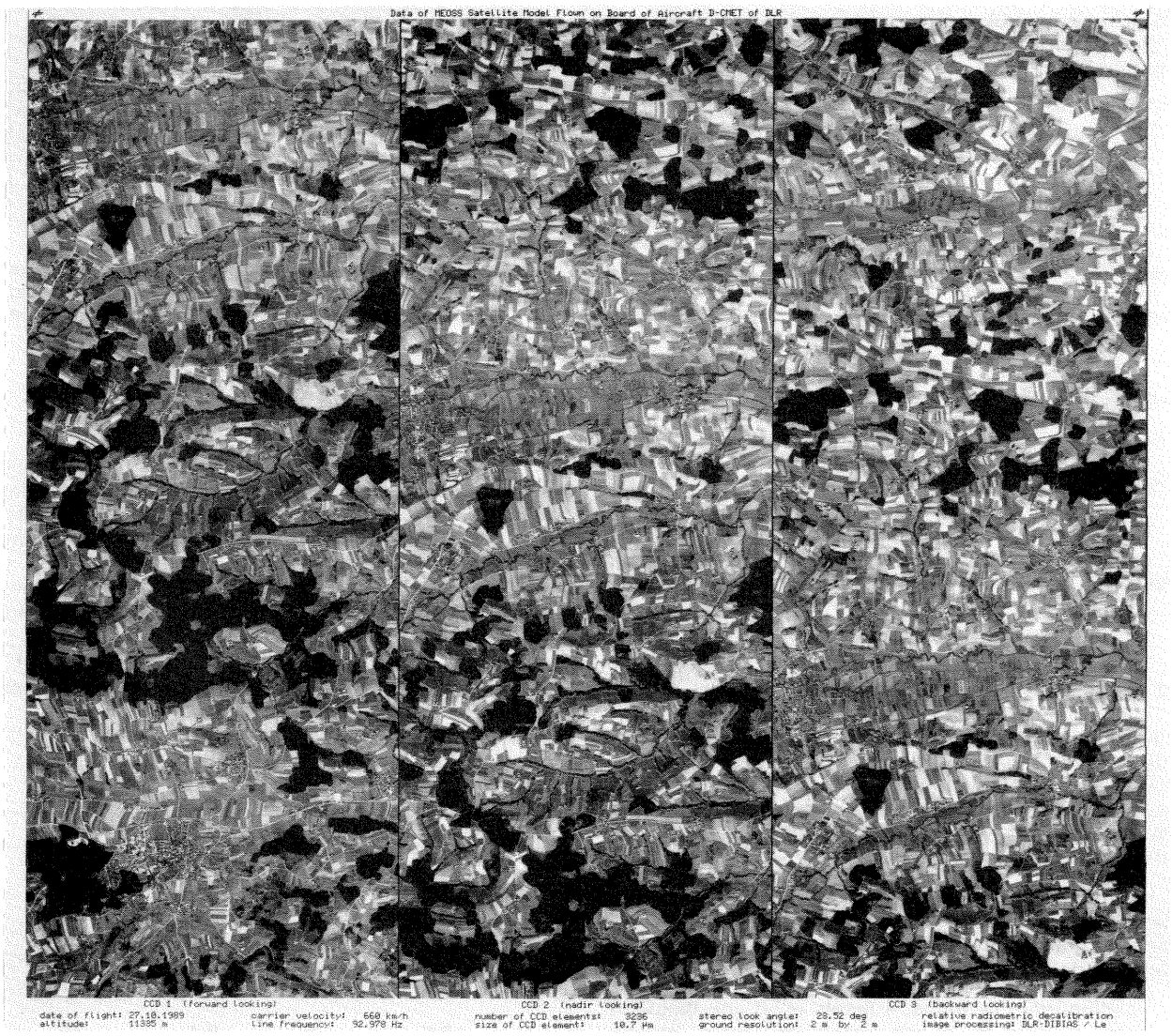

Figure 1. MEOSS Dorfen strip

4. Example: MEOSS airborne data strip Dorfen

4.1 Image material and image matching details

The data strip Dorfen can be seen in Figure 1. The images of the foreward, nadir and backward looking sensors are shown in parallel strips of simultaneously acquired image lines. The along-track displacement between the images of the same objects (one base length) corresponds to about 2400 image lines. The platform, sensor and image parameters are displayed in Table 1.

The numbers of points extracted by the interest operator and being left after the digital image correlation are given in Table 2 for the five levels of the resolution pyramid.

For the manual start at lowest level of resolution 52 and 33 conjugate points were extracted from the backward/nadir and forward/nadir stereo pairs, respectively. The difference in the numbers can be explained by the different information content of the stereo pairs.

Platform Parameters	
ground speed	660 km/h
altitude	11335 m
Sensor Parameters	
objective	Zeiss Biogon
focal length	61.1 mm
stereo angle	23.52 degrees
CCD element size	10.7 micrometer
number of elements per array	3236
line frequency	92.978 Hz
Image Parameters	
ground resolution in flight direction	2 m
ground resolution cross flight	2 m
length of strip	8416 lines / 16.6 km
swath width	3236 pixels / 6.4 km
swath width for triple stereoscopy	3000 pixels / 6.0 km

Table 1. Platform, sensor and image parameters for MEOSS Dorfen strip

The computer time requirement for image matching is about 1/2 day per baselength on modern RISC-type workstations. It could be further reduced by streamlining of the software and - more drastically - by using parallel computing. Both, interest operator and image correlation tasks, can easily be distributed in terms of different image regions to any number of CPUs.

105 ground control and/or check points were measured in the imagery and in maps of scale 1:25000. Their distribution with respect to the nadir imagery is shown in Figure 2 (the case with 20 ground control points is selected).

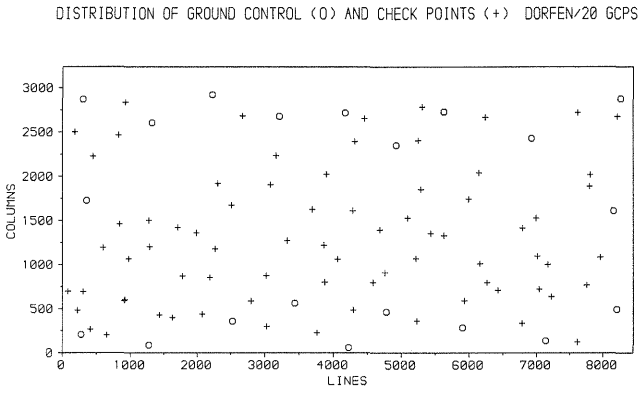

Figure 2. Distribution of ground control and/or check points

4.2 Details on photogrammetric adjustment

The initial values of the exterior orientation were provided by the inertial reference system of the aircraft. The exterior orientation of 120 orientation images have been introduced as unknowns into the adjustment. Figure 3 and Figure 4 show initial and final values of the exterior orientation.

A crucial task in least squares adjustment is the selection of the proper weights for the error equations. For this data strip the following weigths in terms of standard deviations have been used finally:

- collinearity equations: 4 pixels (42.8 μm; included are - besides the image correlation errors - insufficencies in geometric calibration of the camera and the errors introduced by the linear interpolation for the exterior orientation parameters between the orientation images)
- coordinates of ground control points: 20 m
- interior orientation: 10.7 μm
- exterior orientation:
  - position (x,y,z): 100 m, 100 m, 25 m
  - angles (roll, pitch, yaw): 0.02 deg for all
- second order Gauß-Markov process was not used for Dorfen strip

In a first adjustment run using only 1000 conjugate points and relaxed weighting intial estimates for the biases of the exterior orientation have been derived. Later on, 12751 conjugate points have been introduced into the adjustment and the runs were repeated with different numbers of ground control points, varying from 4 to 99. All these adjustment runs converged in two iterations and took about 2 hours CPU-time on IBM 3090, each.

A DEM was generated from the final ground coordinates of the conjugate points by interpolation in the irregular set of points resulting from photogrammetric adjustment. It is given in Figure 5.

level of pyramid	number of interest operator points	number of conjugate points
4	796	552
3	2122	1700
2	5273	4265
1	11871	9109
0	28359	14802

Table 2. Numbers of interest operator and conjugate points on the five levels of the image pyramid for strip Dorfen (reduction in resolution by a factor 2^{level} in line and column directions)

4.3 Error analysis

Theoretical error measures:

To analyse the precision of the results of the adjustment the theoretical standard deviations for the coordinates of all points given by the corresponding coefficients of the inverse of the normal matrix were averaged separately for zones with twofold (zones 1 and 3) and threefold (zone 2) stereoscopic coverage. These values are given in Table 3 for a varying number of ground

zones	$\bar{\sigma}_x$ (m)	$\bar{\sigma}_y$(m)	$\bar{\sigma}_z$ (m)	number of ground control points
1	2.4	1.6	5.5	**99**
2	1.7	1.3	3.2	
3	2.4	1.6	5.2	
all	2.1	1.6	4.4	
1	3.1	1.8	6.0	**40**
2	2.2	1.5	3.8	
3	2.9	1.8	5.7	
all	2.7	1.7	5.0	
1	3.5	1.9	6.4	**30**
2	2.5	1.6	4.3	
3	3.3	1.9	6.0	
all	3.0	1.8	5.4	
1	4.0	2.1	7.0	**20**
2	2.9	1.8	4.9	
3	3.8	2.1	6.5	
all	3.5	1.9	5.9	
1	4.9	2.4	7.8	**10**
2	3.5	2.1	5.7	
3	4.6	2.4	7.4	
all	4.2	2.2	6.8	
1	6.4	3.0	9.9	**4**
2	4.6	2.6	7.6	
3	5.9	3.0	9.4	
all	5.5	2.8	8.8	

Table 3. Average of the theoretical standard deviations for the computed ground coordinates of the conjugate points given for various numbers of ground control points; zone 1 and 3 are the zones with twofold coverage, zone 2 is the area of threefold stereoscopic coverage; the numbers of conjugate points were 4030 for zone 1, 5524 for zone 2, and 3017 for zone 3 (12571 points for all zones)

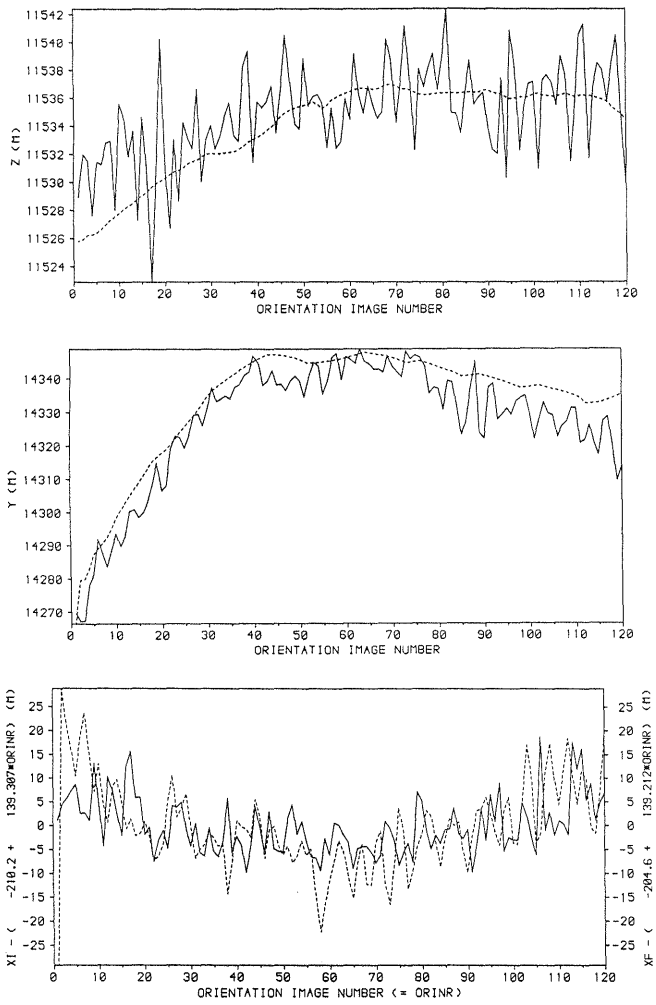

Figure 3. **Initial (dashed lines) and final values of exterior orientation (position part)**; a linear trend is subtracted from x (in flight direction) to make variations from an undisturbed motion visible

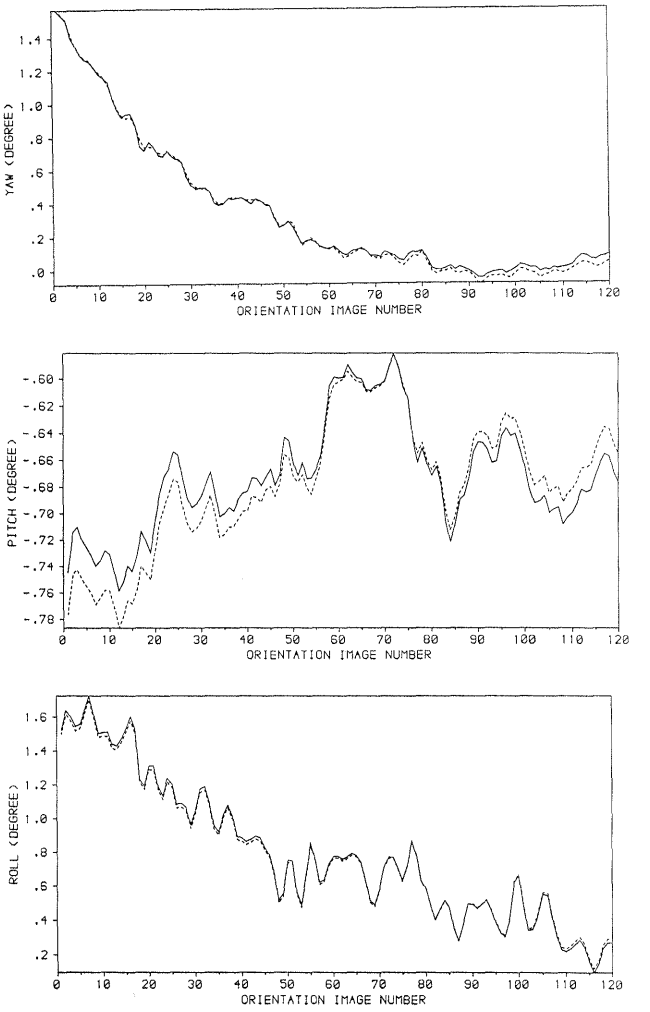

Figure 4. **Initial (dashed lines) and final values of exterior orientation (attitude part)**; the initial attitude values were given by the inertial navigation system of the aircraft and recorded in the housekeeping data of every fourth image line

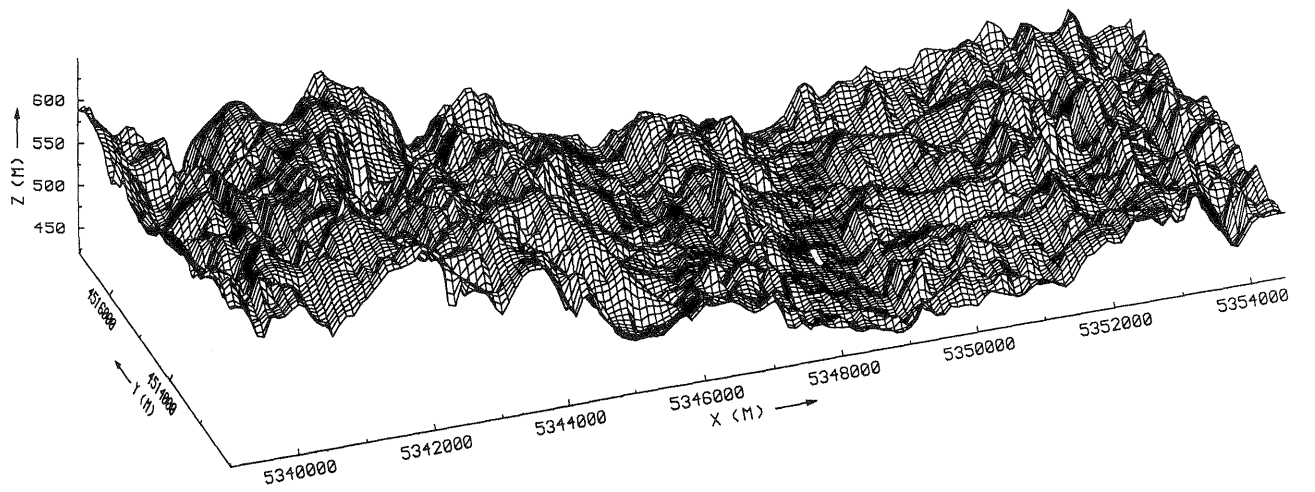

Figure 5. **Digital elevation model resulting from photogrammetric adjustment**

control points. Graphical representations of the dependence of these precision values are shown in Figure 6, Figure 7, and Figure 8 for coordinates x,y,z, respectively. These plots make it evident that not much increase in precision can be gained by increasing the number of ground control points beyond 30.

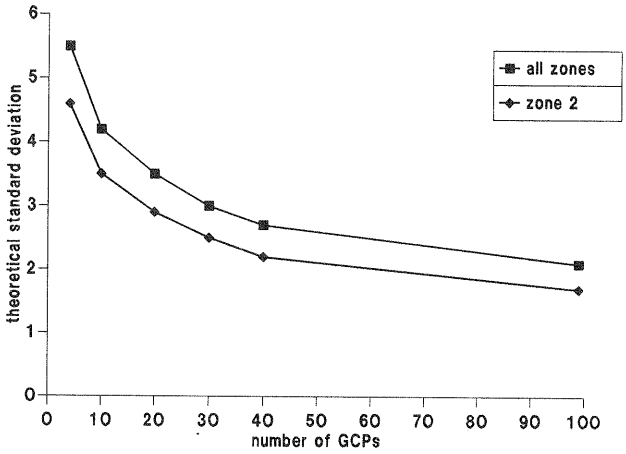

Figure 6. Averaged theoretical standard deviations for coordinate x in dependence on the number of ground control points

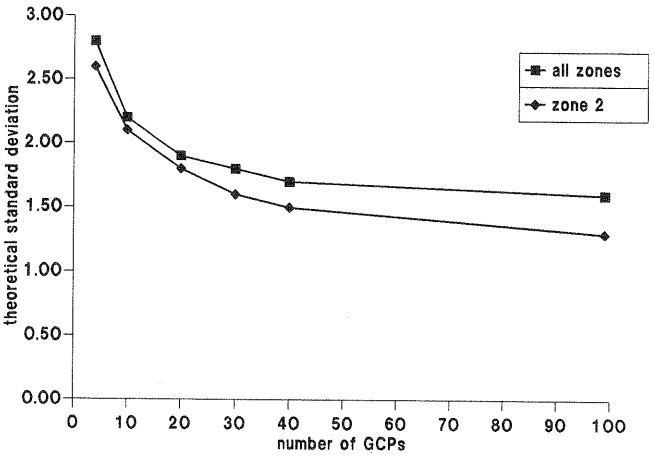

Figure 7. Averaged theoretical standard deviations for coordinate y in dependence on the number of ground control points

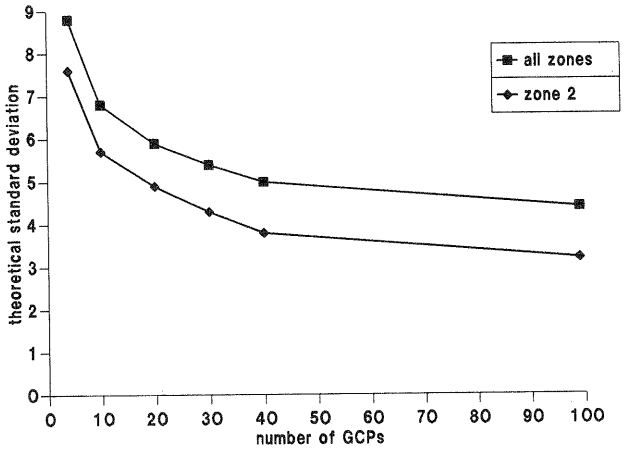

Figure 8. Averaged theoretical standard deviations for coordinate z in dependence on the number of ground control points

Empirical error measures:

As we had 105 ground control points and only a part of them was introduced into the adjustment, the rest has been used as check points. Their ground coordinates were treated as unknowns in the adjustment. Afterwards the rms-differences of the computed and the measured ground coordinates were calculated. The result is shown in Figure 9. The trends are similar to those of the theoretical standard deviations. Of course, the values may be influenced much by the distribution and the number of the check points.

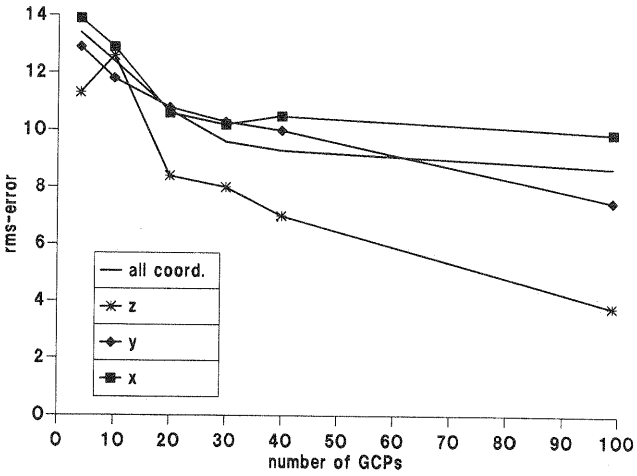

Figure 9. Empirical rms-errors in check points in dependence on number of ground control points

Some more values on the empirical accuracy of the final DEM were derived by comparing it to an already available **DEM of the Bavarian Survey** of that region. This was acquired from the Bayerisches Landesvermessungsamt. Its accuracy is about 2 m and the values are given as a grid with $50m \cdot 50m$ spacing. In order to compare our irregularly distributed results the computed Gauß-Krüger coordinates were taken and bilinear interpolation used to obtain the corresponding height values of the DEM of the Survey. Let us concentrate first on the case with 99 ground control points. Straightforward calculation of the rms differences leads to the first row in Table 4.

However, besides the interpolation errors and the errors in x,y-position this comparison suffers from the fact, that objects found by automatic image matching will include tops of trees and houses. Thus, the number of conjugate points where the computed height is larger than the height derived from the Survey DEM should be higher than the number of points with lower height. This is shown clearly in the last two columns of Table 4. Looking at points with height differences larger than 20m (points excluded in the second row of Table 4) we found that for a substantial number of these points (516 out of 596) the computed height value was larger than the height value in the Survey DEM. A manual classification of these points with height differences larger 20m gave the following result:

Nr. of GCPs	type of points	zone 1 rms diff.	zone 1 nr. of points	zone 2 rms diff.	zone 2 nr. of points	zone 3 rms diff.	zone 3 nr. of points	all zones rms diff.	all zones nr. of points	nr. of points with height > Survey height	nr. of points with height < Survey height
99	all points	9.8	4030	8.3	5524	10.4	3017	9.3	12571	7995	4576
	points with diff. < 20m	7.4	3754	7.4	5386	8.5	2835	7.7	11975	7479	4496
40	all points	11.1	4030	9.2	5524	10.7	3017	10.2	12571	7715	4856
	points with diff. < 20m	8.0	3678	8.2	5357	8.6	2816	8.2	11851	7135	4716
30	all points	11.4	4030	9.1	5524	10.7	3017	10.3	12571	7247	5324
	points with diff. < 20m	8.4	3642	8.1	5363	8.7	2821	8.3	11826	6689	5137
20	all points	12.8	4030	10.4	5524	11.7	3017	11.5	12571	7458	5113
	points with diff. < 20m	8.8	3545	8.9	5233	9.2	2760	9.0	11538	6611	4927
10	all points	15.0	4030	12.1	5524	13.0	3017	13.3	12571	6237	6334
	points with diff. < 20m	9.9	3306	9.9	5030	9.6	2639	9.9	10975	5456	5519
4	all points	15.2	4030	13.8	5524	14.2	3017	14.4	12571	8358	4213
	points with diff. < 20m	9.8	3360	9.6	4634	9.9	2529	9.8	10523	6525	3998

Table 4. rms differences of computed DEM and Survey DEM heights; rms values are given for zones 1,3 of twofold and zone 2 of threefold stereoscopic coverage for all points and for points with absolute value of the height difference less than 20m

- forested areas, trees and built-up areas: 79 %
- other areas (fields,meadows): 12 %
- image matching errors: 9 %

The percentage of matching errors is higher than in the whole set of conjugate points where it was found to be about 4% by manual check. Thus, we believe that the accuracy of the computed DEM will be better than 8m.

Table 4 and Figure 10 in graphical representation for zone 2 show that by varying the number of ground control points a saturation effect can be noticed, here too for numbers beyond 30.

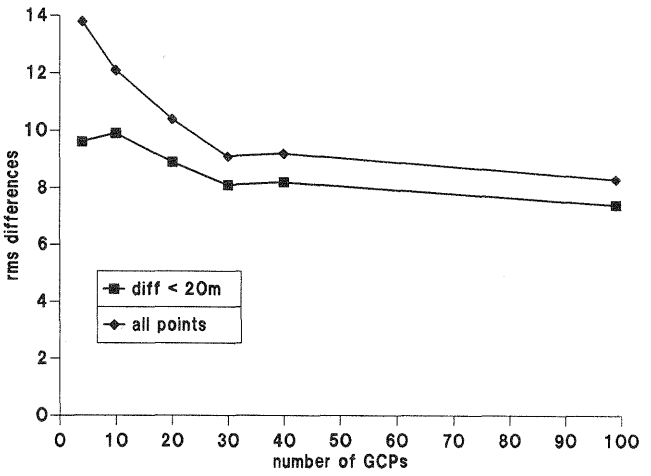

Figure 10. rms-differences to Survey DEM for zone 2 and various numbers of ground control points

5. Conclusions

Software for the derivation of digital elevation models from 3-line scanner imagery has been tested successfully on airborne data of the MEOSS camera. The theoretical standard deviations are in the range of 1-2 pixels and the heights compare well with the Survey DEM. The test was performed under the heavy demands of high resolution of the airborne imagery and rough attitude behaviour of the aircraft. Thus, one can be optimistic for the satellite data of MEOSS and MOMS missions.

Automation of the start of matching in the image pyramid is one of the next goals.

References

<1> **F. Lanzl** *The Monocular Electro-Optical Stereo Scanner (MEOSS) Satellite Experiment*, Progress in Imaging Sensors, ESA SP-525, 1986, pp. 617-620

<2> **J. Wu** *Investigation of Simulated MEOSS Imagery for Sensor Navigation and Terrain Derivation*, Proc. ISPRS Commission I Symposium, Stuttgart 1986, pp. 279-284

<3> **A. Drescher, M. Lehner, J. Wu** *A Common Approach to Navigation and Geometric Image Correction for the Stereoscopic Linescan Camera MEOSS*, Proc. ISPRS Commission I Symposium, Stuttgart 1986, pp. 271-278

<4> **M. Lehner** *Triple Stereoscopic Imagery Simulation and Digital Image Correlation for MEOSS Project*, Proc. ISPRS Commission I Symposium, Stuttgart 1986, pp. 477-484

<5> **M. Lehner, R. Gill** *Photogrammetric Adjustment of Triple Stereoscopic Imagery of an Airborne CCD Scanner* Proc. Optical 3-D Measurement Techniques, Wichmann Verlag, Karlsruhe, 1989

<6> **F. Ackermann, J. Bodechtel, F. Lanzl, D. Meissner, P. Seige, H. Winkenbach, J. Zilger** *MOMS-02/Spacelab D-2: A high resolution multispectral stereo scanner for the second German Spacelab Mission* International Symposium on Optical Engineering and Photonics, April 1-5, 1991, Orlando (USA) (to be published by SPIE)

<7> **C. Heipke, W. Kornus, R. Gill, M. Lehner** *Mapping Technology Based on 3-Line-Camera Imagery*, ISPRS Comm. IV Symposium, May 15-18, 1990, Tsukuba, Japan

<8> **W. Förstner, E. Gülch** *A Fast Operator for Detection and Precise Location of Distinct Points, Corners and Centers of Circular Features*, ISPRS Intercommission Workshop, Interlaken, June 1987

<9> **F. Ackermann** *High Precision Digital Image Correlation* Proceedings of the 39th Photogrammetric Week (1983), Stuttgart University, vol. 9 of the reports of the Institute for Photogrammetry, 1984

<10> **J. Wu** *Geometrische Analyse für Bilddaten stereoskopischer Dreifach-Linearzeilenabtaster*, Dissertation, Wissenschaftliche Arbeiten der Fachrichtung Vermessungswesen der Universität Hannover, Nr. 146, ISSN 0174-1454,1986

<11> **Institut für Kosmosforschung (IKF)** *WAOSS-Experiment for Mars-94 Mission* Phase A Study, Akademie der Wissenschaften der DDR, Berlin, Januar 1990

<12> **DLR Oberpfaffenhofen, Abteilung Planetare Erkundung** *HRSC - High Resolution Stereo Camera / Mars 94 Mission* Consolidated Phase A Conception (Part A: Science Description, DLR-IB 90/3; Part B: Technical Description, DLR-IB 90/4), Oberpfaffenhofen, February 1990